

To be presented at the technical session on
"Heat Transfer to Nuclear Waste Disposal",
ASME Winter Annual Meeting, Chicago, IL,
November 16-21, 1980

LBL-11112

CONF-801102--32

MASTER

BUOYANCY FLOW IN FRACTURES INTERSECTING
A NUCLEAR WASTE REPOSITORY

J.S.Y. Wang and C.F. Tsang

July 1980

Prepared for the U.S. Department of Energy
under Contract W-7405-ENG-48



NOMENCLATURE

b	fracture aperture, m
D	depth of repository, m
g	gravitational constant, m/s^2
i	hydrostatic gradient, m/m
k	permeability, m^2
R	radius of repository, m
T	temperature, °C
v_z	vertical velocity, m/s
v_0	initial horizontal velocity, m/s
x	horizontal coordinate in the east-west direction, m
y	horizontal coordinate in the north-south direction, m
z	vertical coordinate, m
ρ	density, kg/m^3
μ	viscosity $kg/m \cdot s$

INTRODUCTION

Heat released from a nuclear waste repository in a geological formation causes significant temperature changes in the surrounding rock masses. These will in turn heat up groundwater in the formations and induce buoyancy fluid flow. An understanding of the resulting perturbation to the original regional hydrological pattern may be crucial in the determination of repository performance in isolating nuclear waste materials from the biosphere.

In low permeability crystalline rocks, such as granite, groundwater flow is mainly through fractures. For simulation of regional flows, several authors in their calculations approximated the rock formation with multiple fractures by a porous medium model (1-3). In our present study, we adopted a different approach that several major fractures may be important and should be simulated in detail. This is the case if there exist natural faults near the repository, or if there exists a sectionally-connected fracture path which can be represented by a single major fracture. Further, this kind of study may also be used to give a worst-scenario order-of-magnitude result which will provide guidance in our understanding of the problem.

Due to the slow decay of actinides in the nuclear waste and the low thermal conductivity of rocks, the thermohydrological impact of the repository is expected to persist for thousands of years after the emplacement of the wastes. Our simulations are carried out through this time span.

In the following section, the model we used will be described, following which the mathematical approach employed will be indicated. Then calculational results will be presented and discussed.

MODEL IDEALIZATION

In this paper, the nuclear waste repository is idealized to be a flat circular disk with a given time-varying power density dependent on the particular nuclear waste form stored. The repository is assumed to be 1500 m in radius and 500 m below the land surface. Only the case of spent fuel waste is considered and a surface cooling period of 10 years is arbitrarily taken from the time of discharge from a pressurized water reactor to burial in the repository. Nuclear waste density is adjusted so that initial areal power density is 10 W/m^2 . Power decay curve of such a case is given in Figure 1 together with a corresponding curve for reprocessed high level waste for comparison.

Two types of fracture geometry are assumed. The first is a single major fracture vertically intersecting the repository whose axis is in the plane of the fracture. A recharge and a discharge zone are assumed 5 km on either side of the repository. Studies were made of the thermally induced buoyancy flow in the fracture plane and its interaction with natural regional hydrostatic gradient from the recharge to the discharge zones. Three values of hydrostatic gradient were used: 0, 1 and 41, where 1 is a typical value given by

$$i = 0.001 \text{ m/m} \quad (1)$$

i.e., the water level in the recharge zone is 10 m higher than that in the discharge zone. For a fracture with aperture $b = 1 \mu\text{m}$ and a corresponding "parallel-plate" permeability of

$$k = b^2/12 = 8.33 \times 10^{-14} \text{ m}^2, \quad (2)$$

the initial horizontal flow velocity near the land surface (at 20°C) is found to be

$$v_o = \frac{k \rho g}{\mu} i = 8.11 \times 10^{-10} \text{ m/s} = 2.6 \times 10^{-5} \text{ km/yr.} \quad (3)$$

where ρ , μ and g are respectively density, viscosity, and the gravitational constant factor. Results of flow velocities will be presented in unit of v_o .

The second type of geometry studied is that of a two-fracture system. This corresponds to the first type with the addition of one more vertical fracture intersecting the original fracture normally at the repository axis or several distances away from it. Figure 2 shows the case where the two fractures intersect along the axis of the repository as well as the case away from the axis. Studies were made on these models to understand the interaction or interference between two intersecting fracture planes as a function of the intersection locations (one in East-West direction and the other in North-South direction).

In both sets of calculations, the upper boundary is maintained at fixed temperature of 20°C . An ambient geothermal gradient of 30°C/km is assumed. The side boundaries (i.e., recharge or discharge boundary) of each fracture is maintained at hydrostatic pressure and ambient temperature. The lower

boundary at 2 km below the repository and 2.5 km below land surface is a no-flow (closed) boundary.

MATHEMATICAL APPROACH

A numerical model "CCC" developed at Lawrence Berkeley Laboratory (4) was used to study the thermohydrological flow in the fractures. The program "CCC" (which is named after conduction, convection and consolidation) uses an Integrated-Finite-Difference scheme to compute single-phase mass and heat flow in a three-dimensional system in which effects of gravity and temperature-dependent density and viscosity are included. One dimensional theory of Terzaghi is used in this program to calculate land subsidence or swelling. It has been well validated, having been verified against nine analytic or semi-analytic solutions and one field experiment.

Due to the small volume of water present in the fractures (fracture aperture being only of order of μm), the convective contribution to the thermal field is minimal and conduction is the main heat transfer mechanism. Thus the calculation may be carried out in two steps. Firstly conduction calculation was made either by "CCC" or equivalently by a semi-analytical program (5) to obtain the temperature field as a function of time. Then, based on these results, convection in the fractures was calculated by "CCC" to obtain fluid velocities as a function of various key parameters. Fluid velocity is of course what is of particular interest in a waste isolation problem. Values of thermal conductivity for granite of $2.6 \text{ W/m}^\circ\text{C}$ and thermal diffusivity of $1.15 \times 10^{-6} \text{ m}^2/\text{sec}$ are chosen as inputs to our calculations.

Figure 3 displays the mesh design corresponding to one-half of the fracture plane. It is structured to describe best possible heat and flow gradients and to keep the elements to within a reasonable number to optimize computation cost.

INTERACTION OF BUOYANCY FLOW AND REGIONAL FLOW

First let us discuss the temperature field as a function of time after waste emplacement in the repository. Figure 4 displays the temperature vs. depth profile along the axis of the repository for different times after waste burial, the repository being assumed to be fully occupied by waste simultaneously at $t = 0$. Before the waste burial, the profile is a straight line representing a normal original geothermal gradient. At early times the temperature rise is localized near the repository depth. However, after 1000 years, heat from the repository has reached and begun to leak out of the land surface, and a linear temperature profile again is obtained from the land surface to the repository. The vertical temperature gradients, both above and below the repository, drive the buoyancy flow. Radially, the temperature is fairly uniform within the radius of the repository, beyond which the temperature decreases sharply.

To study the interaction of buoyancy flow and regional flow, a single major fracture through the axis of the repository is assumed. The thermally induced flow patterns within the plane fracture after 1000 years are shown in Figure 5 for the case of zero regional hydraulic gradient. In this case

two symmetric convection cells are developed around the edges of the repository. Heated water flows up from the central area of the repository with incoming water drawn from the recharge zones on the two sides 5 km from the repository center and from the ground surface far away from the center of the repository. It is to be noted that large convection cells (i.e., with diameters of same order as the depth of repository) are induced during the life of the repository. This cannot be ignored in considering thermohydrological behavior around a repository.

Figure 6 shows the flow velocities at different times as a function of position on land surface along the length of the fracture. Thus the relative magnitude of the vertical flow velocities near the land surface can be studied. It is seen that these outflow velocities at early times maximize at two symmetric off-center locations, a result of the convective fluid movements. At later times, however, the heat leakage at the surface interferes with the convective flow, and a central maximum develops. The vertical velocities for different times along the axis of the repository are shown in Figure 7. After the initial transient period, the vertical velocities above the repository are approximately independent of depth because of the surface constant-temperature constant-pressure boundary. The zero velocity at depth -2.5 km is due to the imposed no-flow boundary at that depth.

With the presence of regional hydraulic gradient of $i = 0.001$ m/m, the flow patterns are distorted from the symmetric zero-regional-gradient results (Figure 8). On the recharge side (i.e., the side with higher hydraulic head), the regional flow counteracts the horizontal convective movement above the repository and promotes it below the repository. On the discharge side (with lower hydraulic head), the opposite effects occur. The influence of the regional flow on vertical outflow velocities along the length of the fracture is shown in Figure 9. Only a slight suppression of the vertical velocity on the recharge side and a slight increase on the discharge side are observed, indicating a weak coupling of buoyancy and natural regional flows. Figure 10 displays these results for regional gradients of $i = 0, 0.001, \text{ and } 0.004$ m/m at time $t = 1000$ years. The last case for $i = 0.004$ m/m, with a near-surface velocity of $4 v_v$, is approximately equal in magnitude to the vertical outflow velocity at the repository epicenter.

EFFECTS OF FRACTURE-FRACTURE INTERACTION

To investigate the interaction of the buoyancy flows in two intersecting vertical fractures, the geometry similar to that shown in Figure 2 is used. The basic geometry is the same as that of the last section: a plane fracture in the East-West (E-W) direction passing through the axis of the circular-disk repository with or without a regional hydraulic gradient along it. Now a second plane fracture in the North-South (N-S) direction is introduced that intersects normally the first fracture at the axis of the repository or at different distances away from it. The influence on the flow velocities in the first E-W fracture due to this second N-S intersecting fracture is studied here.

The first case considered is when the two vertical fractures intersect at the axis of the repository (case shown in Figure 2). A regional hydraulic gradient of $i = 0.001$ m/m is imposed on E-W fracture, with the recharge and discharge zone assumed at equal distance (5 km) on either side of the repository. The other fracture has zero regional gradient. With such a symmetrical geometry, but different regional flows in the two fractures, the interference is found to be negligible. The flows in the two fractures behave as if they are single fractures. Thus the vertical outflow velocities along the E-W fracture and the N-S fracture are exactly the same as those shown in Figure 9 and Figure 6 respectively. Furthermore, the net recharge drawn from all four sides are equivalent.

However, if the E-W fracture is fixed (i.e., it passes through the repository axis), significant interaction is noticed when the N-S fracture intersects the E-W fracture at locations away from the repository axis. Figures 11, 12, and 13 display the results when the intersection is at $x = -800, -1500, \text{ and } -2000$ meters from repository axis, corresponding to locations within, at, or outside the repository radius. A regional hydraulic gradient is still maintained in the E-W fracture.

The case of $x = -800$ yields results shown in Figure 11. The curves labeled E-W give the vertical velocities along the E-W fracture (i.e., x axis). The location where the N-S fracture intersects it is indicated by the black dot. Thus the intersection point is off center on the x -axis in the E-W direction. The curved labeled N-S give the vertical velocities along the N-S fracture (i.e., y -axis). The black dot on these curves indicates the location where it is intersected by the E-W fracture (x axis). It is always at the point of symmetry in the y direction. In the x - y plane, the two black dots represent the same point and thus should have the same value for vertical velocity. The results for each fracture without the presence of the other are shown as dotted lines. For the present case of $x = -800$ m, i.e., intersection point within the repository radius, only minor interaction is noticed.

For the case of $x = -1500$ m and -2000 m corresponding respectively to intersection locations at the rim of the repository and outside, (Figures 12 and 13), much stronger interaction between the fracture flows occur. This can easily be understood as follows. For the case of $x = 0$, the vertical flow velocities at the intersection point in either fracture in the absence of the other are equal, since, as shown in the last section, effects of regional gradient on vertical velocities are negligible. Thus when the intersection is made, no adjustments in flow velocity are necessary in the common location and the system behaves as independent fractures. On the other hand, for other values of x , the velocities at the intersection point in these fractures in the absence of each other would be quite different, since the temperature fields they experience are quite different. In general, the E-W fracture through the repository axis experiences a much higher temperature rise than the off-axis N-S fracture. Thus when intersection is imposed, much

adjustment in fluid flow velocities occurs. Essentially the N-S fracture acts as an additional recharge to the stronger flow velocities in the E-W fracture. This influences the convection pattern not only locally but globally over large distances.

DISCUSSION

The magnitude of the groundwater flow depends on the fracture system of the rock formation and the driving forces on the groundwater present. The proper characterization of a fractured rock mass is site-specific and an outstanding problem of research. In the present paper we made considerable idealization so that we could focus on two important physical processes: interaction between buoyancy flow and regional hydraulic gradient, and fracture-fracture interference.

The results reported in this paper show that the repository represents a finite-extent heat source which perturbs the original groundwater flow and induces convective movements over thousands of years. The non-isothermal groundwater flow is driven by the hydraulic gradient and the buoyancy force of the heated water relative to the surrounding colder water. Although the gravitational force acts vertically along the z-direction, the development of convective cells around the edges of the repository induces changes in pressure field which in turn couple to the natural horizontal regional gradient. The regional flow slightly suppresses the vertical movement on the recharge side and enhances it on the discharge side. As the wastes heat up the rock formation around the repository, the presence of the ground surface begins to affect the thermally-induced convective movements. Although the regional flow only weakly affects the vertical component of the flow velocity, the addition of the regional horizontal component allow the water particles and radionuclides to flow through possibly longer paths. This, of course, may have important implications in the consideration of radionuclide-rock interactions such as adsorption and dissolution.

The buoyancy flow depends strongly on the available recharge. Intersecting fractures may act as additional recharge paths from one to another with strong influence on fluid flow patterns. This demonstrates the need for careful considerations when one studies single fracture results.

Although the intersecting fracture model used in the present analysis is very simple, it possesses some of the same physical behaviors as that of the more complex fracture systems. This model, complemented with porous medium and other types of models, should provide insight into the dynamics of the thermohydrological flow in fractured rock masses.

ACKNOWLEDGEMENT

Discussions with P.A. Witherspoon and N.G.W. Cook and other colleagues at Lawrence Berkeley Laboratory and the University of California, Berkeley, are appreciated. The work was performed under the auspices of the United States Department of Energy under Contract W-7405-ENG-48.

REFERENCES

- 1 Burgess, A.S., Charlwood, R.G., Skiba, E.L., Ratigan, J.L., Gnirk, P.F., Stille, H., and Lindblom, V.E., "Analyses of Groundwater Flow around a high-level waste repository in crystalline rock," Workshop on Low-Flow, Low-Permeability Measurements in Largely Impermeable Rocks, OECD Nuclear Energy Agency, 1979, Paris, France.
- 2 Dames and Moore, "Technical support for GEIS Radioactive waste Isolation in geologic formations: Groundwater Movement and Nuclide Transport," Y/OWI/TM-36/21, 1978, Office of Waste Isolation Oak Ridge, Tennessee.
- 3 Bourke, P.J., and Hodgkinson, D.P., "Assessment of effects of thermally induced water movement on leakage from a radioactive waste depository," Workshop on Low-Flow, Low-Permeability Measurements in Largely Impermeable Rocks, OECD Nuclear Energy Agency, 1979, Paris, France.
- 4 Lippmann, H.J., Tsang, C.F., and Witherspoon, P.A., "Analysis of the response of geothermal reservoirs under injection and production procedures," SPE 6537, 47th Annual California Regional meeting of the Society of Petroleum Engineers of AIME, 1977, Bakersfield, California.
- 5 Wang, J.S.-Y., Tsang, C.F., Cook, N.G.W., and Witherspoon, P.A., "A study of regional temperature and thermohydrological effects of an underground repository for nuclear wastes in hard rock," LBL-8271, 1979, Lawrence Berkeley Laboratory, Berkeley, California.

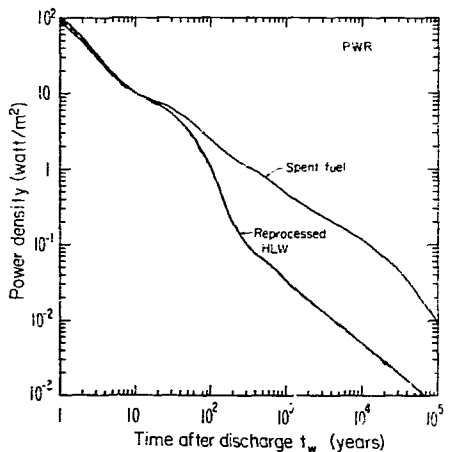


Figure 1. Areal power density of heat generated by the nuclear wastes stored in a repository.

NEL 78110-11362

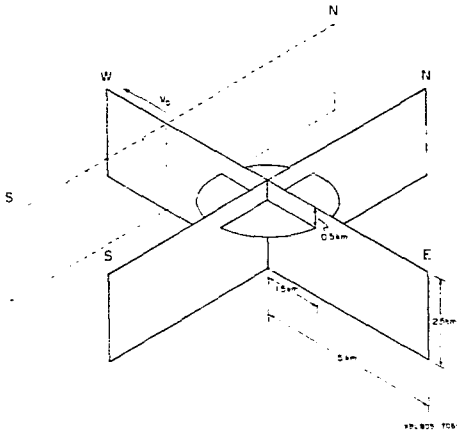


Figure 2. Geometry of two-fracture systems with the E-W fracture (along the regional hydraulic gradient) intersected normally by the N-S fracture at the repository axis (solid N-S fracture) or away from it (dashed N-S fracture).

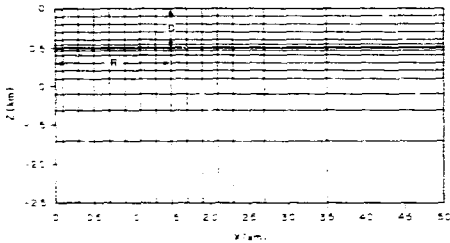


Figure 3. Mesh design corresponding to one-half of the fracture plane.

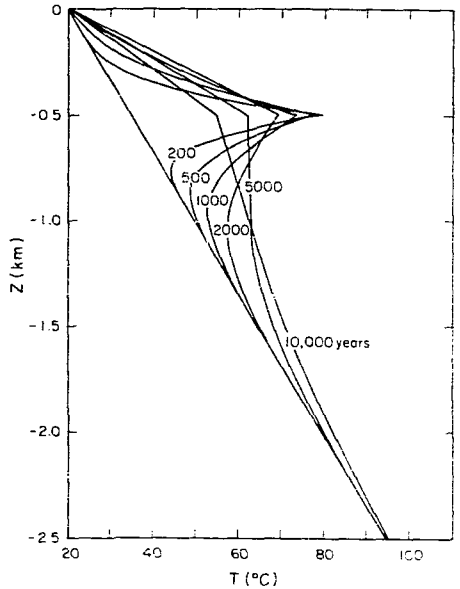


Figure 4. Temperature vs. depth profile along the axis of the repository for different times after waste burial.

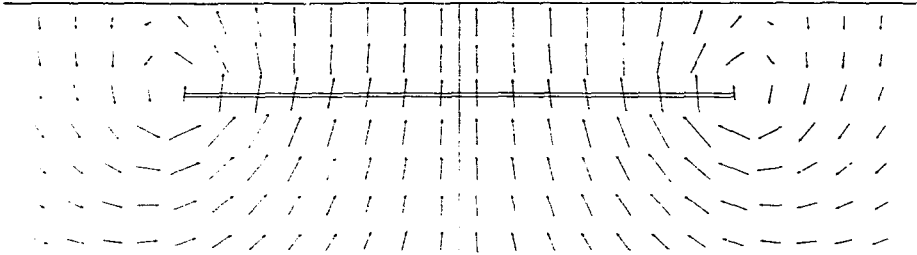


Figure 5. Thermally induced flow patterns within the fracture plane 1000 years after waste burial for the case of zero regional hydraulic gradient.

98-001-11

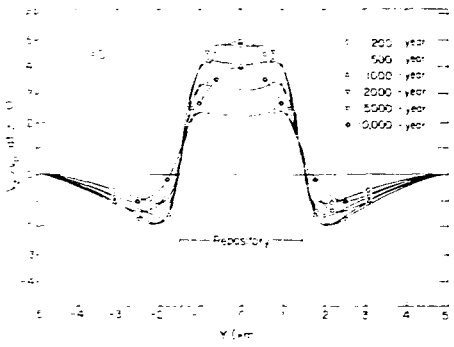


Figure 6. Surface outflow velocities along the length of the fracture at different times for the case of zero regional hydraulic gradient.

98-001-11

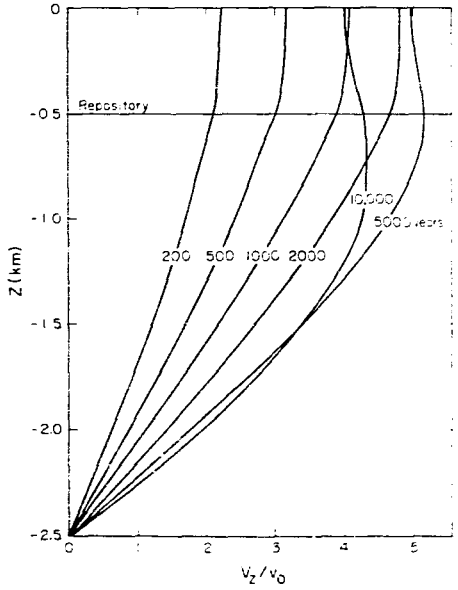


Figure 7. Vertical velocities along the axis of the repository at different times for the case of zero regional hydraulic gradient.

98-001-11

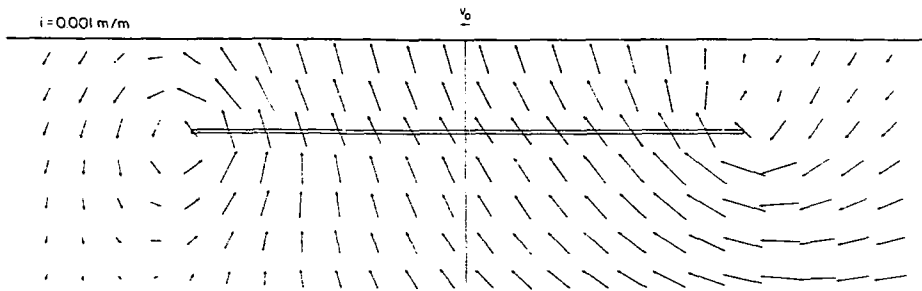


Figure 8. Thermally induced flow patterns with the fracture plane 1000 years after waste burial for the case with regional hydraulic gradient $i = 0.001$ m/m.

HL 800-7010

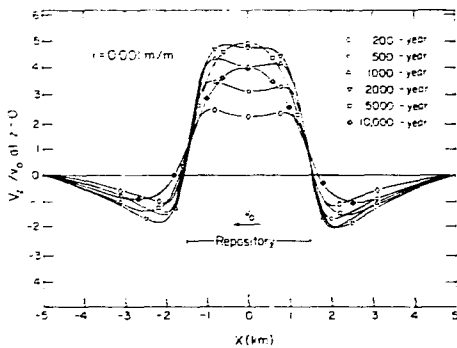


Figure 9. Surface outflow velocities along the length of the fracture at different times for the case with regional hydraulic gradient $i = 0.001$ m/m.

HL 801-941

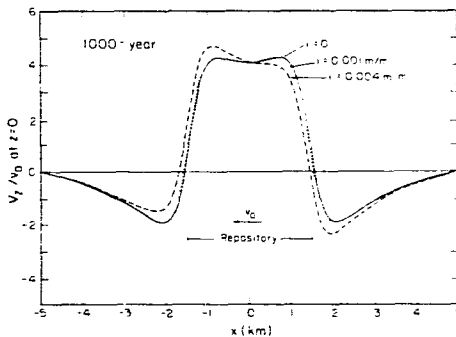


Figure 10. Effects of different regional hydraulic gradient i on the surface outflow velocities along the length of the fracture at 1000 years after waste burial.

HL 801-7070

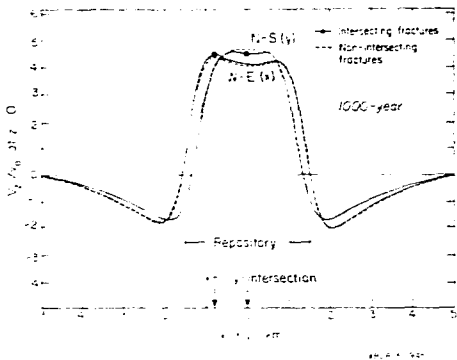


Figure 11. Surface outflow velocities at 1000 years along the length x of the E-W fracture and the length y of the N-S fracture. The fracture-fracture intersection is located at $x = -800$ m and $y = 0$ within the repository radius.

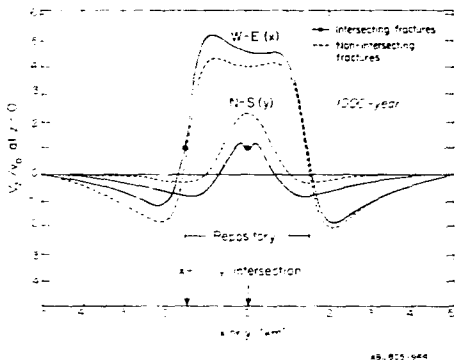


Figure 12. Surface outflow velocities at 1000 years, along the length x of the E-W fracture and the length y of the N-S fracture. The fracture-fracture intersection is located at $x = -1500$ m and $y = 0$ through the rim of the repository.

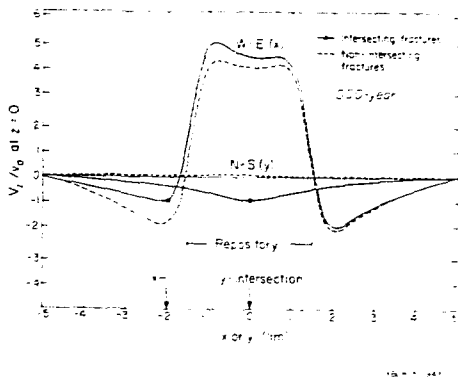


Figure 13. Surface outflow velocities at 1000 years along the length x of the E-W fracture and the length y of the N-S fracture. The fracture-fracture intersection is located at $x = -2000$ m and $y = 0$ outside the repository radius.